



Hot Deformation Behavior and Strain Rate Sensitivity of 33MnCrB5 Boron Steel Using Material Constitutive Equations

Emre Teker¹ · Mohd Danish² · Munish Kumar Gupta³  · Mustafa Kuntoğlu⁴ · Mehmet Erdi Korkmaz¹ 

Received: 13 June 2021 / Accepted: 10 November 2021 / Published online: 2 December 2021
© The Author(s) 2021

Abstract In this paper, the constitutive equation parameters (Johnson–Cook parameters) of the 33MnCrB5 material were determined with the help of tensile tests. Initially, Johnson–Cook (JC) model was used for performing the simulations of the sample with finite element analysis with the help of ANSYS software. For these operations, the sample was first used at a certain temperature (24 °C) and low strain rates (10^{-1} , 10^{-2} , 10^{-3} s⁻¹) and quasi-static tensile tests were performed. Then, high temperature tensile tests were performed with strain rate values of 10^{-3} s⁻¹ at temperatures of 300 °C, 600 °C, and 900 °C, respectively. Finally, JC parameters belonging to test materials were found in accordance with the results obtained from the high temperature tensile and quasi-static tests. In the last stage, the results obtained from the

simulation software for the yield stress, maximum stress, and elongation values were compared with the experimental results. As a result, deviation values for quasi-static tests are calculated as 5.04% at yield stress, 5.57% at maximum stress, and 5.68% at elongation, while for high temperature, yield stress is 9.42%, maximum stress is 11.49% and the elongation value is 7.63%. The accuracy of JC parameters was verified with the comparison made with the obtained data.

Keywords 33MnCrB5 boron steel · Johnson–Cook parameters · Stress–strain · High temperature · Finite element analysis

1 Introduction

33MnCrB5 steel is achieved by adding a small amount of boron to medium carbon steels. Boron steels exhibit an equivalent hardenability with high carbon steels and expensive low alloy steels [1–4]. Steels with greater passive safety, lower weight, and higher strength values are increasingly being employed in the production of various automobile parts [5]. As a result, it is important to establish the suitable area conditions for the automobile industry's parts. The only method used in the production of open sections of steel parts with very high strength value is the hot forging process of boron steels [6, 7].

Recently, the application of finite element tensile and compression test simulation tools have been increased because experimental investigations take a long time and have a significant cost of implementation [8, 9]. For this reason, modeling of plastic deformation processes with the finite element (FE) method offers an alternative method [10–14]. However, to prove that the material is appropriate

✉ Munish Kumar Gupta
munishguptanit@gmail.com

Emre Teker
emreteker0490@gmail.com

Mohd Danish
mdanish@uj.edu.sa

Mustafa Kuntoğlu
mkuntoglu@selcuk.edu.tr

Mehmet Erdi Korkmaz
merdikorkmaz@karabuk.edu.tr

¹ Department of Mechanical Engineering, Karabük University, Karabük, Turkey

² Department of Mechanical and Materials Engineering, University of Jeddah, Jeddah 21589, Saudi Arabia

³ Faculty of Mechanical Engineering, Opole University of Technology, 76 Proszkowska St, 45-758 Opole, Poland

⁴ Mechanical Engineering Department, Technology Faculty, Selcuk University, 42130 Konya, Turkey

and applicable, the constitutive equation parameters of the material must be determined exactly and the material model must be selected correctly [15–17]. Zerilli–Armstrong, JC model and its modified version are extensively preferred for FE analysis programs [18–21]. For the determination of the Johnson–Cook model, quasi-static and high temperature experiments need to be performed [22–24]. Several studies were performed to determine the JC material model parameters. In this context, Sahu et al. determined the JC parameters for AA1100 aluminum alloy verifying it with finite element simulations [25]. Korkmaz et al. determined the JC model parameters for the Nimonic 80A alloy and verified it with finite element simulation [26]. Naderi et al. investigated the mechanical features of steels with and without boron additives and determined that the investigated properties of boron added steels were higher than the steels without boron added. [27]. Zhao et al. researched the mechanical properties of Q235 low carbon steel with and without boron additive after hot forming, and they determined that Q235 steel with boron additive showed a stronger hot ductility than the other. [3]. After conducting the literature review, it was observed that there were many studies on the machinability and modeling of boron steels [28, 29]. However, due to the lack of a material model on 33MnCrB5 alloy steel, a study on deformation processes could not be found. Research on machining takes a long time and is expensive in terms of cost. Hence, numerical modeling has been used as an alternative method in modeling cutting processes. FE model is a frequently used numerical method in the plastic deformation process [30–32]. ANSYS, ABAQUS, DEFORM, etc. software is very useful in predicting cutting forces, temperatures, and stresses in the plastic deformation process. In addition, such analysis programs make a significant contribution to the realization of transactions at low costs. Owing to these advantages, the FE method is preferred for many authors in engineering problems and analysis of manufacturing processes. The results obtained from the simulations in which FE modeling is made and the results obtained in the plastic deformation process (temperature, force, etc.) should match each other [33–37]. For this reason, accurate modeling is of great importance in simulation softwares. Correct modeling means that the results to be obtained are accurate and realistic. The most appropriate constitutive material model from which correct modeling parameters can be obtained is the JC material model. The material models in the material library of the simulation software are used in most of the simulation studies. Within the scope of the study, the main purpose is to determine the JC material model parameter of the 33MnCrB5 alloy material, which is not found in the literature. Afterward, the created material model parameters will be adapted to the simulation software, and tensile tests

will be simulated under quasi-static and high temperature tensile tests. In the last stage, to determine the applicability level, the experimental findings and the findings obtained from the simulation software were compared and evaluated. This research will not only fill the gap in the literature but also contribute to the automotive industry.

2 Materials and Methods

33MnCrB5 steel containing high strength boron additive was used as the test material. It was delivered as two pieces of 33MnCrB5 steel with the dimensions of $\varnothing 20 \text{ mm} \times 900 \text{ mm}$ for use in high temperature and quasi-static tensile tests. The chemical composition of 33MnCrB5 boron steel is demonstrated in Table 1.

To specify the material parameters of JC for 33MnCrB5 boron steel, quasi-static and high temperature tensile tests were conducted. The samples prepared from 33MnCrB5 test material were first tested as quasi-static tensile tests at room temperature (24 °C) and low strain rates (10^{-1} , 10^{-2} , 10^{-3} s^{-1}). Then, they were exposed to high temperature tensile tests at 300 °C, 600 °C, and 900 °C at reference strain rate (10^{-3} s^{-1}), respectively. The sample size used for quasi-static and high temperature tensile tests are given in Fig. 1.

The images of the samples prepared for the tensile tests are shown in Fig. 2a. The images of the fractured samples as a result of the quasi-static and high temperature tensile tests are given in Fig. 2b and c, respectively.

The tensile tests were carried out as per TS EN ISO 6892–1 and TS 206 standards. The Zwick/Roell Z600 Universal tensile-compression test setup at Karabuk University Iron-Steel Institute was used and the image of the tensile test device is given in Fig. 3.

3 Determination of JC Parameters

Johnson–Cook model is the method used to calculate the strengths of the material depending on the unit strain value, unit strain rate, and temperature [38]. Unlike other models, the Johnson–Cook model is extensively used in high strain rate deformations because it is semi-empirical and easier to determine the mechanical behaviors of the model. The yield stress (σ) is expressed in Eq. 1.

$$\sigma = [A + B\varepsilon^n] \left[1 + C \ln \left(\frac{\dot{\varepsilon}}{\varepsilon_0} \right) \right] [1 - (T^*)^m] \quad (1)$$

Here $[A + B\varepsilon^n]$ gives isothermal stress as a function of strain at the lowest strain rate; $\left[1 + C \ln \left(\frac{\dot{\varepsilon}}{\varepsilon_0} \right) \right]$ gives the effect of strain rate and $[1 - (T^*)^m]$ gives thermal effects.

Table 1 The chemical composition of 33MnCrB5

C	Si	Mn	P	S	Cr	Ni	Mo	Al
0.36	0.245	1.30	0.017	0.0022	0.299	0.103	0.0531	0.0216
Cu	Co	Ti	V	W	Pb	B	Sn	Fe
0.223	0.0074	0.0425	0.0016	0.0067	0.0013	0.0015	0.0151	97.3

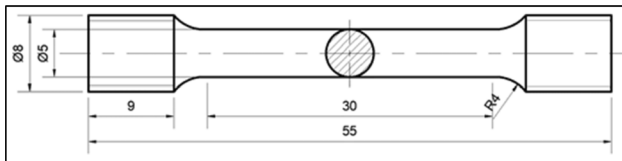


Fig. 1 The dimensions of quasi-static and high temperature tensile test specimen (mm)

$$T^* = \frac{T - T_r}{T_m - T_r} \tag{2}$$

Here, T_r and T_m are the reference temperature and the melting temperature, respectively.

4 Results and Discussions

4.1 “A, B and n” Parameters

The constants (A , B , and n) used in the equation are found from the stress–strain curve obtained at the reference strain rate and room temperature. Also, T^* can be expressed as Eq. 2.

The “A” parameter in the material model gives the yield stress at the reference strain rate (10^{-3} s^{-1}). The yield stress value determined for room temperature and reference strain rate ($24 \text{ }^\circ\text{C}$ and 10^{-3} s^{-1}) according to the test

Fig. 2 a The samples prepared for quasi-static and high temperature tensile tests. **b** The samples fractured at room temperature ($24 \text{ }^\circ\text{C}$) and 10^{-1} , 10^{-2} , 10^{-3} s^{-1} strain rates. **c** The samples fractured at reference strain rate (10^{-3} s^{-1}) for temperatures of 300 , 600 and $900 \text{ }^\circ\text{C}$



(a)



(b)



(c)

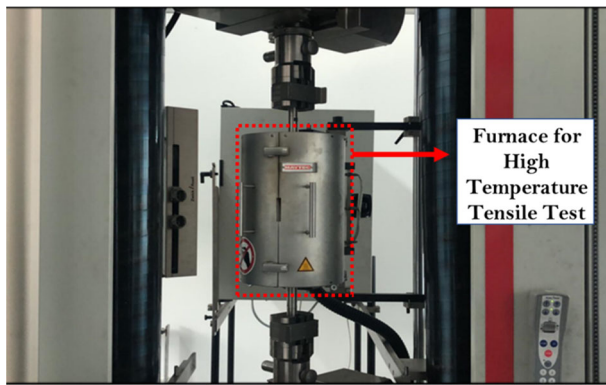


Fig. 3 Zwick/Roell Z600 Universal tensile-compression test setup

results performed as per the given standards is 627 MPa. The yield stress value is obtained by using the graphic in Fig. 4.

In the experiments, the yield point has to be assumed as zero strain for the calculation of B and n parameters. Then, B and n constants are determined depending on the increase in elongation and stress values. By using the necessary equations of the true stress–strain curve and the engineering stress–strain curve quasi-static tensile test result was obtained. It has been seen in Fig. 4 that yield points of engineering and real stress–strain curves are the same. According to Fig. 4, the strain values at 2.5%, 5%, 7.5%, and 10% stress values have been determined to be 838, 927, 970, and 991 MPa, respectively. These determined average stress–strain values are used in the equation specified in Eq. 3 at certain strains, and the B constant is 916 MPa and the n constant is 0.333.

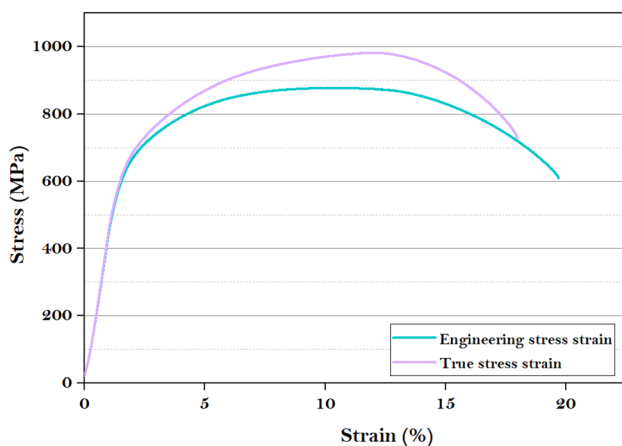


Fig. 4 Stress–strain graph obtained as a result of the tensile test performed under room temperature and reference strain rate (24 °C and 10^{-3} s^{-1})

$$\sigma^0 = (A + B(\dot{\epsilon}^p)^n) \quad (3)$$

4.2 “C” Parameters

The “C” parameter required to create a JC material model shows the strain rate constant. The changes in the stress values with the increase in strain rates can be depicted as shown in Fig. 5. In determining the “C” parameter, only yield points are taken as criteria. Therefore, only engineering stress–strain curves have been created.

According to the tensile tests performed at 10^{-1} , 10^{-2} , 10^{-3} s^{-1} strain rates at room temperature (24 °C), it is observed that yield stress is 627, 632, and 638 MPa, respectively. This situation shows that the increase in the strain rates also increases the yield stress values. The same trend is followed in the literature [39–41]. The graph shown in Fig. 6, is created by using the equation specified in Eq. 4. From the graph obtained, the C constant is calculated as 0.0032.

$$\sigma = \sigma^0 \left(1 + C \ln \left(\frac{\dot{\epsilon}^p}{\dot{\epsilon}_0} \right) \right) \quad (4)$$

4.3 “m” Parameter

Tensile tests performed at high temperatures are used for dynamic applications. Thus, there is a continuous elevation in dislocation density and a noticeable decrease in tensile strength due to the material being affected by high temperatures. “m” parameter in the JC material model refers to the temperature constant. In the process of determining the “m” parameter in the Johnson–Cook material model, its appropriate to use temperatures of 900 °C and less. Figure 7 shows the stress–strain graph for four different temperature values (24 °C, 300 °C, 600 °C, and 900 °C) in

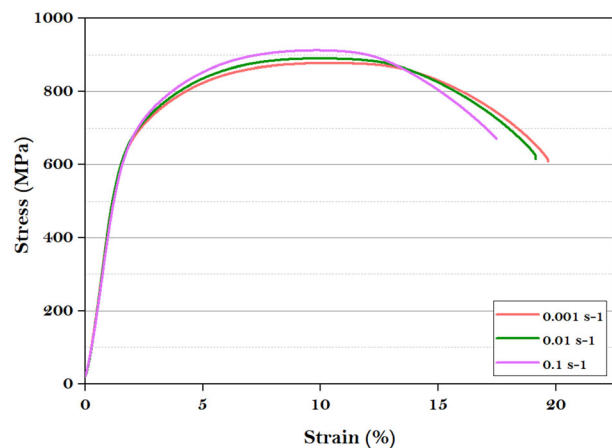


Fig. 5 Stress–strain graph obtained as a result of the tensile test performed at 10^{-1} , 10^{-2} , 10^{-3} s^{-1} strain rates at room temperature (24 °C)

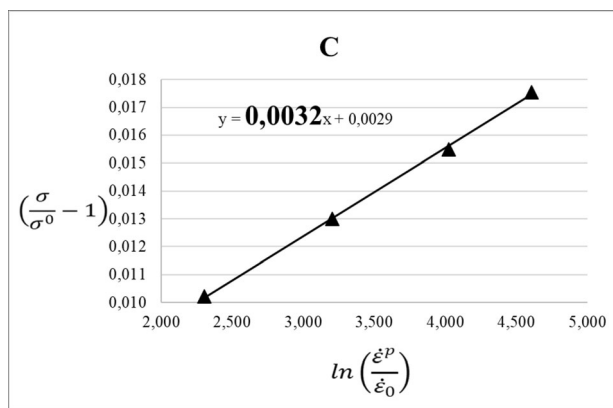


Fig. 6 Logarithmic relationship for determining “C” parameter

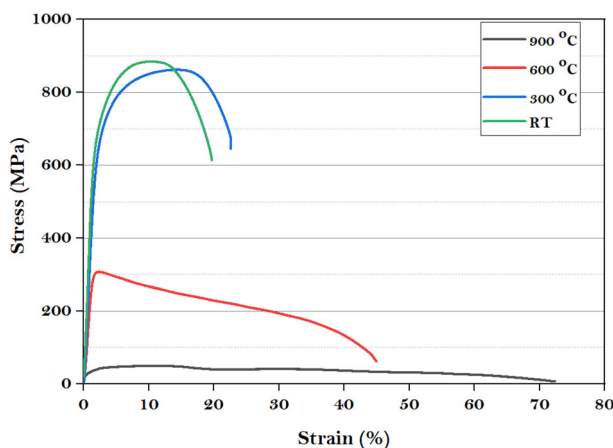


Fig. 7 Stress–strain graph for 24 °C, 300 °C, 600 °C and 900 °C temperature at reference strain rate (10^{-3} s^{-1})

the tests performed at the reference strain rate (10^{-3} s^{-1}). Only the yield points have been taken in the Johnson–Cook material model for determining the “m” parameter. Therefore, only engineering stress–strain curves are created.

From Fig. 7, it can be seen that the yield stresses of the material at 24 °C, 300 °C, 600 °C, and 900 °C temperature

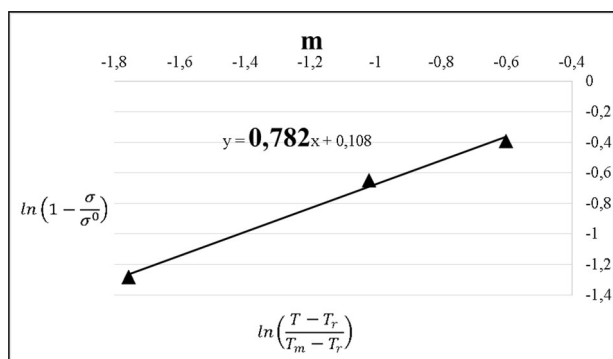


Fig. 8 Logarithmic relationship for determining “m” parameter

values have been determined as 627, 593, 287 and 32 MPa, respectively. The graph in Fig. 8 is created by using the equation specified in Eq. 5. The “m” constant is found to be 0.782 from the obtained graph.

$$\sigma = \sigma^0 \left(1 - \left(\frac{T - T_r}{T_m - T_r} \right)^m \right) \tag{5}$$

JC parameters created for 33MnCrB5 boron steel after quasi-static and high temperature tensile tests are given in Table 2.

5 Comparison of Experimental and Simulation Results

With the help of quasi static and high temperature tensile tests, JC material parameters of 33MnCrB5 steel have been determined. Then the tensile test simulations in ANSYS have been performed by adapting these JC parameters. After simulating the quasi-static tensile tests, the images of the fractured samples for both simulation and experimental are given in Fig. 9.

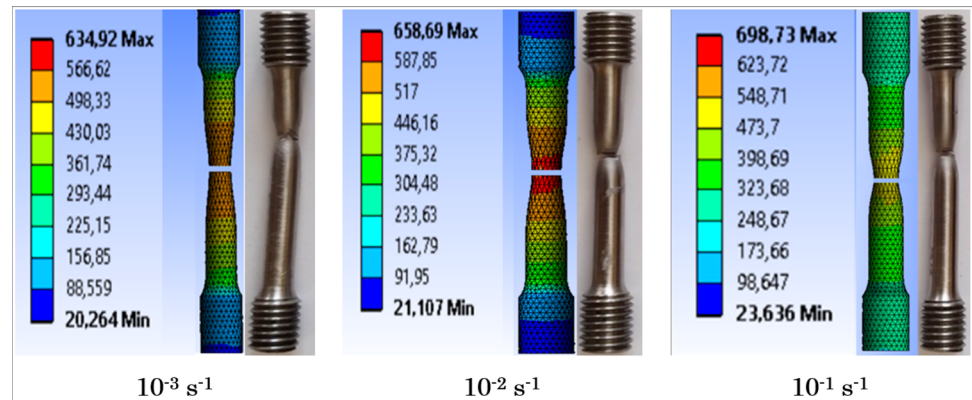
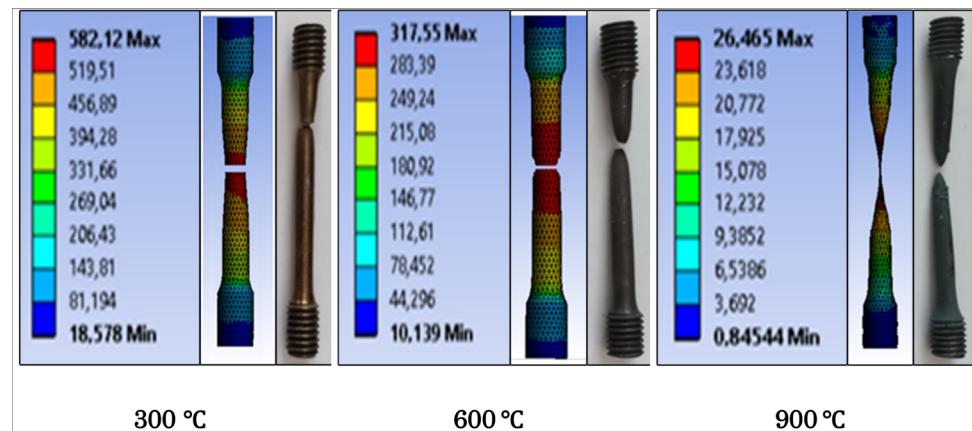
As a result of tensile test simulations performed at room temperature (24 °C) and strain rates of 10^{-1} , 10^{-2} , 10^{-3} s^{-1} , respectively, the yield stresses have been determined as 635 MPa, 659 MPa and 699 MPa. The images of the fractured samples because of high temperature tensile tests simulations are given in Fig. 10.

As a result of the tensile test simulations performed at the reference strain rate (10^{-3} s^{-1}) and temperatures of 300 °C, 600 °C and 900 °C, respectively, the yield stress is determined as 582 MPa, 318 MPa and 27 MPa. The results obtained from the tensile tests simulations performed for quasi-static and high temperature values are given in comparison with the results obtained from experimental studies. When the results are examined, yield stress is obtained as 627 MPa, 632 MPa and 638 MPa at strain rates of 10^{-1} , 10^{-2} , and 10^{-3} s^{-1} , respectively. In the finite element analysis, it is found as 635 MPa, 659 MPa and 699 MPa, increased by 1.28%, 4.27% and 9.56%, respectively.

In experimental studies, the maximum stress has been measured as 887 MPa, 890 MPa, and 904 MPa, respectively at strain rates of 10^{-1} , 10^{-2} , and 10^{-3} s^{-1} . In the finite element analysis, it is obtained as 913 MPa, 934 MPa and 984 MPa thus increasing by 2.93%, 4.94% and 8.84% respectively. Elongation values are obtained as 19.67%, 19.14% and 17.47%, respectively, at strain rates of at 10^{-1} , 10^{-2} , and 10^{-3} s^{-1} in experimental studies. In the finite element analysis, it is found to be 20.29%, 20.27% and 18.87%, an increase by 3.15%, 5.90% and 8.01%, respectively.

Table 2 Johnson–Cook material parameters for 33MnCrB5 boron steel

Material	A (MPa)	B (MPa)	n	C	m	$\dot{\epsilon}_0$ (s^{-1})
33MnCrB5	627	916	0.333	0.0032	0.782	10^{-3}

Fig. 9 Experiment and simulation fractures at strain rates of 10^{-3} , 10^{-2} , $10^{-1} s^{-1}$ **Fig. 10** Experimental and simulation fractures obtained at 300 °C, 600 °C and 900 °C temperatures

After the evaluation of the results, a deviation of 5.04% in the yield stress, 5.57% in the maximum stress, and 5.68% in the elongation value has been found between the simulation results and experimental results. The simulation result with the stress–strain graphs obtained from the experimental results for the 33MnCrB5 boron steel at strain rates of 10^{-3} , 10^{-2} , $10^{-3} s^{-1}$, respectively are shown in Fig. 11a–c, respectively. The resulting stress–strain graphs are shown comparatively.

When the results are examined, yield stress is obtained as 593 MPa, 287 MPa and 32 MPa, respectively, for 300 °C, 600 °C, and 900 °C temperatures in experimental studies conducted under high temperature. The results obtained from the finite element analysis deviate by 1.85%, 10.80%, and 15.62%, respectively, and are found to be 582 MPa, 318 MPa, and 27 MPa. Maximum stresses measured in experimental studies for temperatures of 300 °C, 600 °C, and 900 °C, respectively are 917 MPa,

307 MPa, and 50 MPa. The results obtained from the finite element analysis deviate by 2.94%, 19.54%, and 12%, respectively, and are determined as 890 MPa, 367 MPa and 44 MPa. Elongation values are obtained in experimental studies as 22.57%, 44.92%, and 72.32% for temperatures of 300 °C, 600 °C, and 900 °C, respectively. The results obtained from the finite element analysis deviate by 5.98%, 5.52%, and 11.40% and are obtained as 23.92%, 47.40%, and 80.57%. When all the values obtained have been evaluated, it is determined that between the simulation results performed in the finite element analysis and the results obtained from the experimental studies, there is a 9.42% deviation for the yield stress, 11.49% for the maximum stress, and 7.63% for the elongation value. In comparison, although the yield stress for the 300 °C, temperature is low, the deviation at the maximum stress and elongation values is low, but it is a little bit high for the 600 °C and 900 °C temperature values. The reason is that,

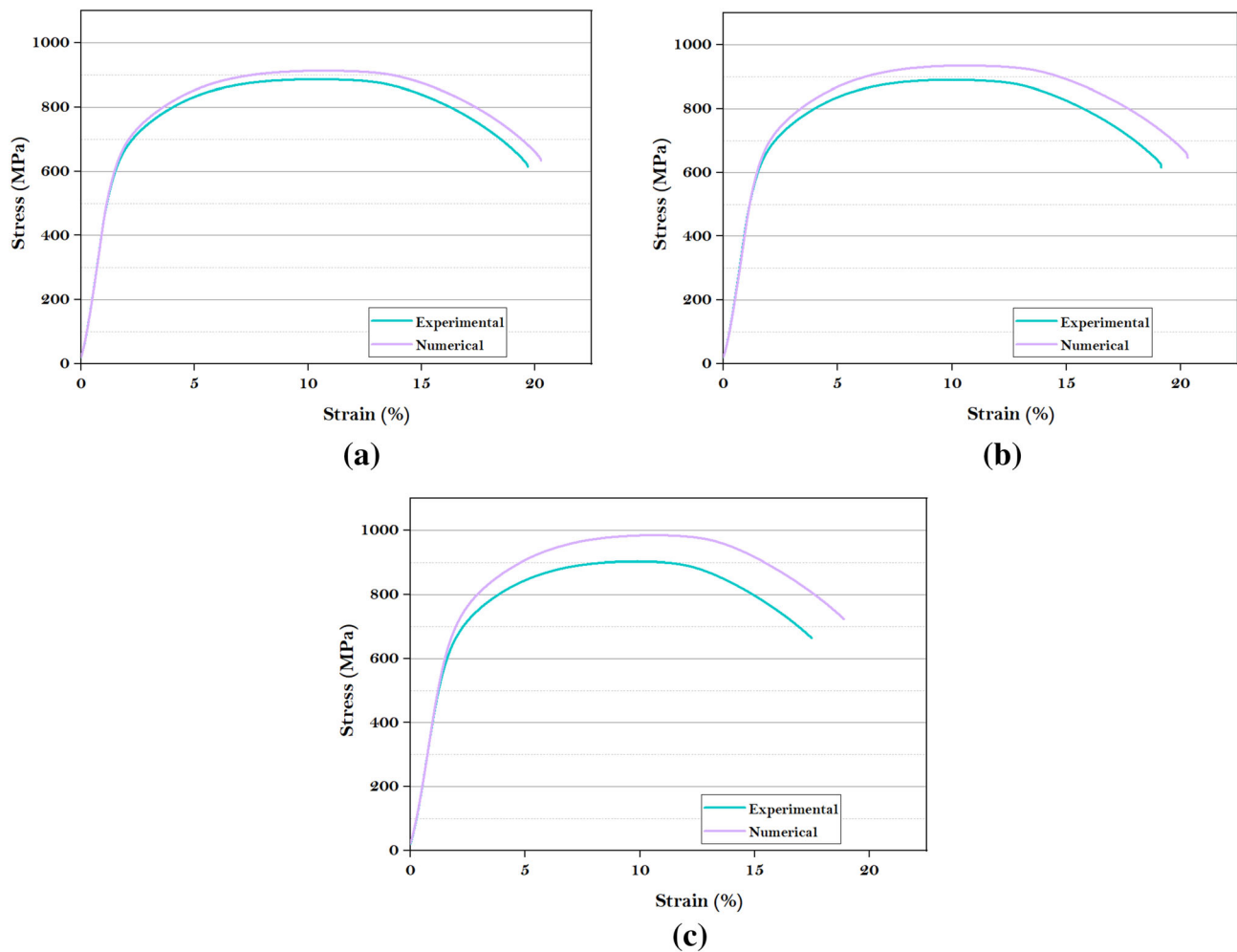


Fig. 11 Comparisons of experimental and simulation results for **a** 10^{-3} s^{-1} , **b** 10^{-2} s^{-1} and **c** 10^{-1} s^{-1}

the FE software cannot consider all microstructural changes such as changing of grain sizes or boundaries, twinning, phase transformation, etc. However, the temperature constant (m), which is one of the J–C parameters, and calculated based on the yield stress obtained from the test results and so this deviation can be ignored.

In Fig. 12a–c, the stress–strain graphs obtained from the experimental and simulation results for 33MnCrB5 boron steel at temperatures of 300 °C, 600 °C and 900 °C, respectively, are shown.

6 Evaluation of SEM Observations

6.1 Quasi-static Evaluations

When Fig. 11 is examined, the amount of the strain at failure demonstrated by the material from the tensile stress to the failure point demonstrates that the material has a ductile structure. Furthermore, the material's significant

plastic deformation and huge quantity of absorbed energy support the idea that it has a ductile structure [42]. SEM analyses on broken test materials have also been used to investigate the ductility or brittleness conditions. Figure 13 shows the SEM analyses acquired from the inspection of the sample fracture surface following the quasi-static tensile test performed at room temperature (24 °C) and a strain rate of 10^{-3} s^{-1} .

According to the SEM analysis evaluated for the strain rate of 10^{-3} s^{-1} in Fig. 13, it has been noticed that the sample has undergone a ductile fracture under quasi-static effect. Because of the unhindered dislocation motions, the grains find a specific moment for elongation and exhibit high toughness. The dimples are also noticeable. As a result, the material exhibits a high degree of plastic deformation. Moreover, cleavage planes are formed in the sample, tested under quasi-static effect, as expected from ductile material.

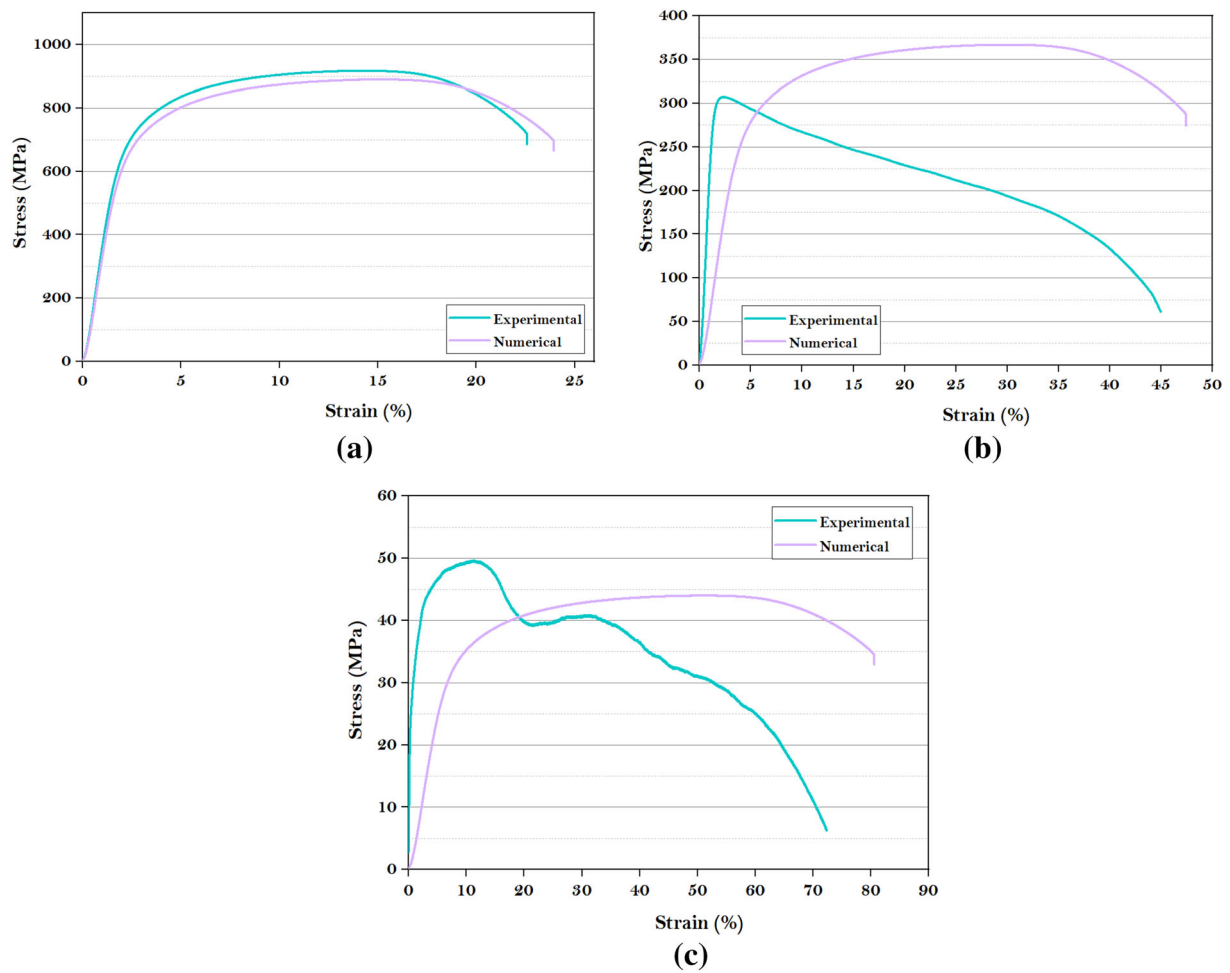


Fig. 12 Comparisons of experimental and simulation results for **a** 300 °C, **b** 600 °C and **c** 900 °C

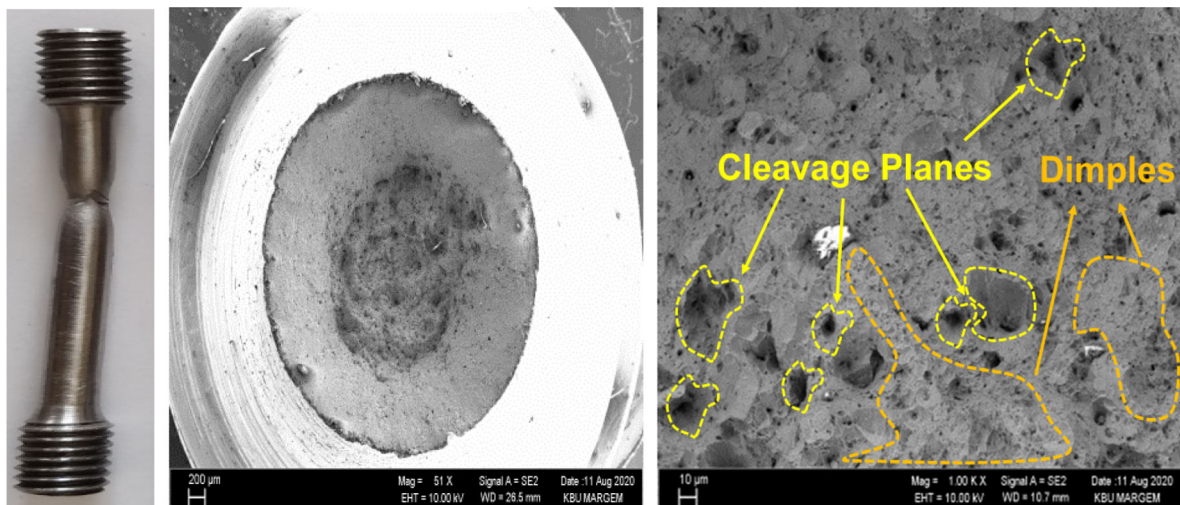


Fig. 13 SEM analysis performed at the strain rate of 10^{-3} s^{-1}

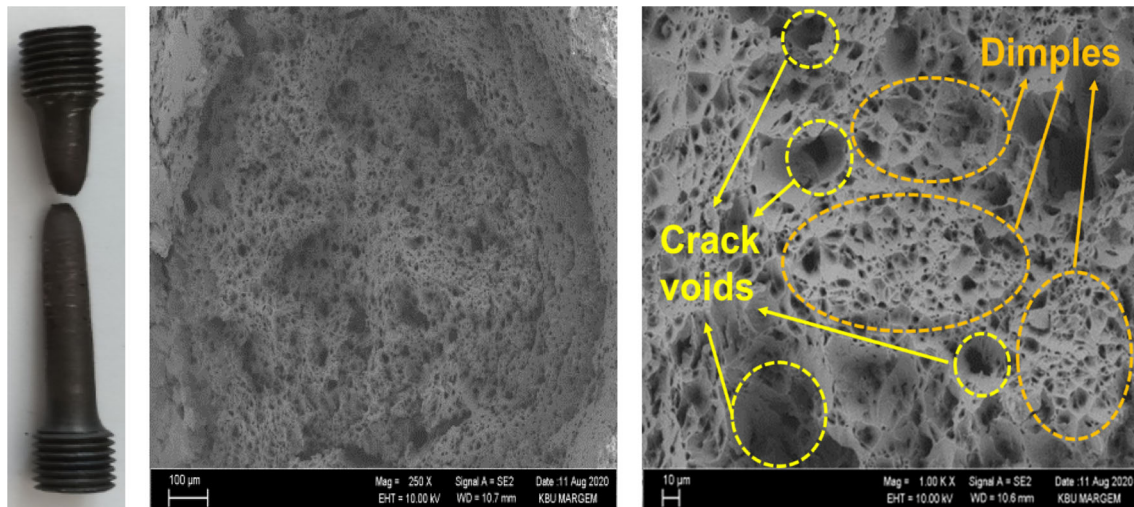


Fig. 14 SEM analysis performed at the temperature of 600 °C

6.2 High Temperature Evaluations

Figure 12 shows that the material has a ductile structure. Furthermore, the ductility or brittleness conditions have been investigated using SEM analysis on broken test materials. Figure 14 shows an SEM examination of the sample fracture surface taken after a tensile test at the reference strain rate and temperature of 600 °C.

High temperature values have an effect on ductility as well as softness. As a consequence of the experimental and modeling investigations, the samples soften at high temperatures, and the elongation values rise as well [43]. Though, ductile fractures arise following the development and merging of cracked voids, as indicated in the literature [44]. SEM study done for a temperature of 600 °C shows the development of fractured voids Fig. 14. Furthermore, the samples are broken with a complicated structure because of the high temperature deformation.

7 Conclusions

The material constitutive equation (Zerilli Armstrong, Johnson–Cook, etc.) must be discovered in the ANSYS software, which is a FE program, in order to model the plastic deformation processes of the material. Recently, while doing any plastic deformation analysis in finite element analysis tools, material constitutive equations have been employed in the literature. The goal of this work is to discover the material constitutive equation of 33MnCrB5 boron steel, and add to the literature. For the purpose of the research, quasi-static and high temperature plastic deformation simulations for 33MnCrB5 boron steel were performed in the ANSYS analysis software utilizing structural

equation parameters acquired from experimental studies. As a result of the simulations performed,

- The yield stresses were acquired as 627 MPa, 632 MPa, and 638 MPa, respectively, at strain rates of 10^{-1} , 10^{-2} , 10^{-3} s $^{-1}$ in experimental studies. In the FE analysis, they were observed as 635 MPa, 659 MPa, and 699 MPa, rising by 1.28%, 4.27%, and 9.56%, respectively.
- The yield stresses were obtained as 593 MPa, 287 MPa, and 32 MPa, respectively, for 300 °C, 600 °C, and 900 °C temperatures in experimental studies performed at high temperatures. The results obtained from the FE analysis diverged by 1.85%, 10.80%, and 15.62%, respectively, and were observed as 582 MPa, 318 MPa, and 27 MPa.
- MAPE was calculated as 5.04% for the yield stress, 5.57% for the tensile stress, and 5.68% for the elongation value between the quasi-static tensile tests and FE simulations.
- MAPE was calculated as 9.42% for the yield stress, 11.49% for the tensile stress, and 7.63% for the elongation value between the high temperature tensile tests and FE simulations.
- The correctness of JC parameters of 33MnCrB5 boron steel was demonstrated by comparisons between experimental and simulation findings. It is known that when the plastic deformation analysis of this steel is done at low strain rates and high temperatures in future, the parameters acquired within the scope of the study will be used.
- It has been suggested for future studies that JC material model parameters of 33MnCrB5 boron steel can be determined by using other material models (Zerilli–

Armstrong, modified JC, etc.) and compared with JC parameters.

- Obtained JC parameters can be compared with ANSYS software packages by subjecting tensile tests in different simulation programs based on the finite element method.

Acknowledgments This study is supported by Scientific Research Project Unit of Karabük University (FDT-2019-2063), and the authors express their appreciation for this support.

Open Access This article is licensed under a Creative Commons Attribution 4.0 International License, which permits use, sharing, adaptation, distribution and reproduction in any medium or format, as long as you give appropriate credit to the original author(s) and the source, provide a link to the Creative Commons licence, and indicate if changes were made. The images or other third party material in this article are included in the article's Creative Commons licence, unless indicated otherwise in a credit line to the material. If material is not included in the article's Creative Commons licence and your intended use is not permitted by statutory regulation or exceeds the permitted use, you will need to obtain permission directly from the copyright holder. To view a copy of this licence, visit <http://creativecommons.org/licenses/by/4.0/>.

References

- Ganapathy M, Li N, Lin J, and Bhattacharjee D, *Int J Light Mater Manuf* **3** (2020) 277.
- Kapil A, Thurston B, Vivek A, and Daehn G, *Manuf Lett* **25** (2020) 30.
- Zhao J, Zhu H, Wang W, Wang L, and Wang W, *Results Phys* **15** (2019) 102813.
- Tang B, Wang Q, Guo N, Liu J, Ge H, Luo Z, and Li X, *Eng Fract Mech* **240** (2020) 107351.
- Yurtkuran H, Korkmaz M E, and Günay M, *Gazi Univ J Sci* **29** (2016) 987.
- Åkerström P, Wikman B, and Oldenburg M, *Model Simul Mater Sci Eng* **13** (2005) 1291.
- Li C, and Xie S, *Vacuum* **170** (2019) 108960.
- Sharma S, Singh J, Gupta M K, Mia M, Dwivedi S P, Saxena A, Chattopadhyaya S, Singh R, Pimenov D Y, and Korkmaz M E, *J Mater Res Technol* **12** (2021) 1564.
- Erden M A, Yaşar N, Korkmaz M E, Ayvaci B, Nimel Sworna Ross K, and Mia M, *Int J Adv Manuf Technol* **114** (2021) 2811.
- Ijaz H, Asad M, Danish M, Gupta M K, Siddiqui M E, and Al-Zahrani A, *Int J Adv Manuf Technol* **114** (2021) 1991.
- Teng X, Huo D, Chen W, Wong E, Zheng L, and Shyha I, *J Manuf Process* **32** (2018) 116.
- Yang J, Wang X, and Kang M, *J Manuf Process* **31** (2018) 768.
- Korkmaz M E, and Yaşar N, *J Prod Syst Manuf Sci* **2** (2021) 50.
- Günay M, Korkmaz M E, and Yaşar N, *Mechanika* **23** (2017) 432.
- Venkata Ramana A, Balasundar I, Davidson M J, Balamuralikrishnan R, and Raghu T, *Trans Indian Inst Met* **72** (2019) 2869.
- Ijaz H, Danish M, Asad M, and Rubaiee S, *Mech Ind* **21** (2020) 615.
- Rasaei S, and Mirzaei A H, *Trans Indian Inst Met* **72** (2019) 1023.
- Dorogoy A, and Rittel D, *Exp Mech* **49** (2009) 881.
- Korkmaz M E, Verleysen P, and Günay M, *Trans Indian Inst Met* **71** (2018) 2945.
- Danish M, Ginta T L, Habib K, Abdul Rani A M, and Saha B B, *Heat Transf Eng* **40** (2019) 1023.
- Korkmaz M E, *Trans Indian Inst Met* **72** (2019) 2663.
- Shokry A, *J Mater Eng Perform* **26** (2017) 5723.
- Farahani H K, Ketabchi M, and Zangeneh S, *J Mater Eng Perform* **26** (2017) 5284.
- Xu H, Zhao B, Lu X, Liu Z, Li T, Zhong N, and Yin X, *J Mater Eng Perform* **28** (2019) 6958.
- Sahu S, Pada Mondal D, Dass Goel M, and Zahid Ansari M, *Mater Today Proc* **5** (2018) 5349.
- Korkmaz M E, Günay M, and Verleysen P, *J Alloys Compd* **801** (2019) 542.
- Naderi M, Ketabchi M, Abbasi M, and Bleck W, *Proc Eng* **10** (2011) 460.
- Cao X, Li Z, Zhou X, Luo Z, and Duan J, *Measurement* **171** (2021) 108766.
- Kasana S S, and Pandey O P, *Mater Today Commun* **26** (2021) 101959.
- Korkmaz M E, and Günay M, *Arab J Sci Eng* **43** (2018) 4863.
- Korkmaz M E, and Günay M, *J Polytech* **22** (2019) 41.
- Korkmaz M E, *J Mater Res Technol* **9** (2020) 6322.
- Yadav R K, Abhishek K, and Mahapatra S S, *Simul Model Pract Theory* **52** (2015) 1.
- Şerban D A, Marsavina L, Rusu L, and Negru R, *Arch Appl Mech* **89** (2018) 1.
- Yaşar N, *J Mech Sci Technol* **33** (2019) 4771.
- Neto D M, Simões V M, Oliveira M C, Alves J L, Laurent H, Oudriss A, and Menezes L F, *Mech Mater* **146** (2020) 103398.
- Zhang J F, Zhang X X, Wang Q Z, Xiao B L, and Ma Z Y, *Mech Mater* **122** (2018) 96.
- Danish M, Ginta T L, Habib K, Carou D, Rani A M A, and Saha B B, *Int J Adv Manuf Technol* **91** (2017) 2855.
- Sun X, Zhao K, Li Y, Huang R, Ye Z, Zhang Y, and Ma J, *Constr Build Mater* **158** (2018) 657.
- Gong D, Nadolski S, Sun C, Klein B, and Kou J, *Powder Technol* **339** (2018) 595.
- Wang W, Zhang X, Chow N, Li Z, and Shi Y, *Compos Struct* **200** (2018) 135.
- Sivasankaran S, and Al-Mufadi F, *Trans Indian Inst Met* **73** (2020) 1439.
- He H, Yi Y, Cui J, and Huang S, *Vacuum* **160** (2019) 293.
- Mallikarjuna Rao P, and Bhattacharya S S, *Trans Indian Inst Met* **62** (2009) 41.

Publisher's Note Springer Nature remains neutral with regard to jurisdictional claims in published maps and institutional affiliations.